Molecular BioSystems

Cite this: *Mol. BioSyst.*, 2011, **7**, 2480–2489

www.rsc.org/molecularbiosystems

PAPER

Identification of secondary effects of hyperexcitability by proteomic profiling of myotonic mouse muscle†

Lisa Staunton,[a] Harald Jockusch,[b] Christiane Wiegand,[c] Timo Albrecht[b] and Kay Ohlendieck*[a]

Received 2nd February 2011, Accepted 11th May 2011
DOI: 10.1039/c1mb05043e

Myotonia is a symptom of various genetic and acquired skeletal muscular disorders and is characterized by hyperexcitability of the sarcolemma. Here, we have performed a comparative proteomic study of the genetic mouse models ADR, MTO and MTO*5J of human congenital myotonia in order to determine myotonia-specific changes in the global protein complement of gastrocnemius muscle. Proteomic analyses of myotonia in the mouse, which is caused by mutations in the gene encoding the muscular chloride channel *Clc1*, revealed a generally perturbed protein expression pattern in severely affected ADR and MTO muscle, but less pronounced alterations in mildly diseased MTO*5J mice. Alterations were found in major metabolic pathways, the contractile machinery, ion handling elements, the cellular stress response and cell signaling mechanisms, clearly confirming a glycolytic-to-oxidative transformation process in myotonic fast muscle. In the long-term, a detailed biomarker signature of myotonia will improve our understanding of the pathobiochemical processes underlying this disorder and be helpful in determining how a single mutation in a tissue-specific gene can trigger severe downstream effects on the expression levels of a very large number of genes in contractile tissues.

Introduction

A distinct group of skeletal muscular disorders is represented by ion channelopathies. These diseases of the voluntary contractile system are characterized by recurrent patterns of mutations, whereby primary abnormalities in Cl^--, Na^+-, K^+- or Ca^{2+}-channels are associated with hyperexcitability causing myotonia, hypoexcitability leading to periodic paralysis, or susceptibility to the pharmacogenetic disorder malignant hyperthermia.[1] The subgroup of myotonias and paramyotonias is classified as hereditary muscle diseases in which involuntary contractions are caused by hyperexcitability of the muscle fibre plasmalemma.[2] Hyperexcitability can be caused either by lowered Cl^--conductance (myotonias) or by prolonged activity of Na^+-channels (paramyotonias).[3] Nondystrophic myotonias are closely related to ion channel dysfunction, and are classified as channelopathies affecting muscle-specific Cl^-- or Na^+-channels.[4] Mutations in the gene encoding the muscle Na^+-channel are associated with paramyotonia congenita, potassium-sensitive myotonia and hyperkalemic periodic paralysis with myotonia. In contrast, nondystrophic chloride channelopathies are responsible for myotonia congenita, recessive Becker myotonia and dominant Thomsen myotonia.[5]

Genetic animal models of neuromuscular diseases are widely used for studying the molecular pathogenesis of inherited disorders, evaluating the effects of drug treatment on disease progression and testing of novel therapeutic strategies such as stem cell transfer or gene therapy.[6] In the case of myotonia research, the muscle-specific manifestation[7] and molecular basis[8] of this disorder has been clarified by the analysis of a myotonic mouse mutant,[9] the ADR mouse (phenotype ADR, genotype $Clc1^{adr/adr}$).[10] Myotonia in the mouse is caused by insertional (allele *adr*[8]), nonsense (allele *mto*[11]) or missense (allele *adr*K*)[11] mutations at the gene locus *Clc1* (chromosome 6) for the muscular chloride channel ClC-1. In human myotonia, a large number of both recessive (type Becker) and dominant (type Thomsen) mutations at the gene locus *CLCN1* (chromosome 7) have been identified.[4] The myotonic ADR and MTO mice are both genocopies and phenocopies of human congenital myotonias. The more pronounced phenotype makes them ideal model systems for studying secondary effects of myotonia on the skeletal muscle proteome. However, it is important to keep in mind that mice exhibit a higher prevalence of fast-glycolytic fibres in the majority of muscles as compared to humans.

[a] *Department of Biology, National University of Ireland, Maynooth, Co. Kildare, Ireland. E-mail: kay.ohlendieck@nuim.ie; Fax: +353 1 708-3845; Tel: +353 1 708-3842*
[b] *Developmental Biology and Molecular Pathology, University of Bielefeld, Bielefeld, Germany*
[c] *Biochemistry III, Faculty of Chemistry, University of Bielefeld, Bielefeld, Germany*
† Electronic supplementary information (ESI) available. See DOI: 10.1039/c1mb05043e

Prior to the molecular elucidation of mouse myotonias, a variety of biochemical changes have been described in affected muscles[10,12] that represent downstream effects of the hyperexcitability of myotonic muscle.[13–18] Many of these biochemical changes were reminiscent of those observed in chronic low-frequency stimulated fast muscle[19] which involves a fibre type shift from fast-glycolytic white muscle to fast-oxidative red muscle.[13,14] In long-term electrostimulated fast rabbit muscles, fibre transitions eventually result in a slow-oxidative muscle phenotype that is reflected by extensive fast-to-slow switches in protein isoforms.[19] In myotonic muscles, transformations are well documented by the alterations in the isoform expression pattern of slow and heavy chains of muscle myosins. For example, hyperexcitability triggers a reduced phosphorylation of the fast myosin light chain MLC2f[14] and a lower concentration of myosin heavy chain isoform MyHC-IIB in myotonic fast muscles.[18] However, since previously documented changes in myotonic mouse muscle have been established by classical histochemical, protein biochemical, immunological and mRNA quantification methods, these technologies may have overlooked more subtle changes in the global protein pattern. In this respect, mass spectrometry-based proteomics suggests itself as a large-scale and high-throughput analytical tool to complement traditional biochemical and histochemical studies of myotonic animal models.

Here, we have carried out a comparative proteomic survey of ADR *vs.* MTO muscle preparations. In addition we have included the characterization of a new allele, *mto*5J*, at the *Clc1* locus of the mouse which allows for a longer survival of the affected homozygous animals. The milder phenotype of MTO*5J mice is clinically closer to human congenital myotonia. In the present work we have attempted a broad proteomics-based analysis to determine a more complete spectrum of changes caused by a single, well defined gene mutation by means of a changed physiological activity of the organ in which this gene is expressed, skeletal muscle. Comparative immunoblotting of the myotonic muscles from the animal models ADR, MTO and MTO*5J confirmed previously reported myotonia-specific changes and proteomic profiling revealed a generally perturbed protein expression pattern in the severely affected ADR and MTO muscle, but less pronounced alterations in mildly diseased MTO*5J mice. The proteomic identification of hitherto undetected changes contributes to an improved understanding of the overall pathobiochemical processes in myotonic muscle.

Materials and methods

Materials

Electrophoresis-grade chemicals, immobilized pH gradient strips of pH 4–7 and pH 6–11, IPG buffers for isoelectric focusing and acetonitrile were purchased from Amersham Biosciences/GE Healthcare (Little Chalfont, Bucks., UK). Acrylamide stock solutions were obtained as ultrapure protogel mixtures from National Diagnostics (Atlanta, GA, USA). Protein molecular weight standards, Laemmli-type gel buffers, Coomassie Blue dye and Bradford reagent for protein quantification were from Biorad Laboratories (Hemel-Hempstead, Herts., UK). Protease inhibitors and chemiluminescence substrate were purchased from Roche Diagnostics (Mannheim, Germany). Ruthenium batho-phenanthrolinedisulfonate chelate for the production of RuBPs dye was from Reagecon Diagnostic Limited (Shannon, Ireland). Sequencing grade-modified trypsin was obtained from Promega (Madison, WI, USA). LC-MS Chromasolv water and formic acid were from Fluka (Dorset, UK). Nitrocellulose transfer stacks were obtained from Invitrogen (CA, USA). X-Ray film was from Fuji Photo Film (Tokyo, Japan). Antibodies were purchased from Abcam, Cambridge, UK (ab7785 to tropomyosin; ab11427 to parvalbumin; ab2480 to the phosphorylatable form of myosin light chain; ab28777 to the voltage-dependent ion channel VDAC1; ab48003 to myosin light chain MLC2), Sigma, Dorset, UK (M8648 to myoglobin), Upstate Biotechnology, Lake Placid, NY (mAb 05-298 to α-dystroglycan) and Affinity Bioreagents, Golden, CO, USA (MA3912 to fast SERCA1 Ca^{2+}-ATPase; MA3919 to slow/cardiac SERCA2 Ca^{2+}-ATPase). All secondary antibodies were from Chemicon International (Temecula, CA, USA). Ponceau S-Red staining solution, DNase-I and all general chemicals were obtained from Sigma Chemical Company (Dorset, UK).

Genetic mouse models of myotonia

Three allelic mutations at the gene locus *Clc1* coding for the muscular chloride channel ClC-1 were used in this study: Mice carrying the *adr* allele ($Clc1^{adr}$) have been obtained from Dr D. L. Watts, Guy's Hospital, London in 1982; the mutation was on the A2G background; SWR/J mice carrying the *mto* allele ($Clc1^{mto}$) were purchased from Jackson Laboratory (Bar Harbor, Maine, USA) in 1986, whereby the mutation was subsequently bred into the C57Bl/6 strain. The *mto5J* allele ($Clc1^{mto-5J}$) was discovered at Jackson Laboratory in 2000 during a mutant screen on a 129 background, and allelism to *mto* was shown. In the University of Bielefeld, the mutation was transferred to a C57/BL6 background. Originally, this strain carried a $Fcgr2b^{tm1Ttk}$ (Fc gamma2b receptor = CD32) transgene, which was later removed by controlled breeding. Allele *adr* is due to a transposon insertion in intron 12^{8} which disrupts normal splicing; *mto* to a stop codon in codon 47 (R47X);[11] *mto5J* carries a base insertion in codon 75 which causes a frameshift resulting in a stop codon in position 93. As expected, all three alleles are null mutations that do not produce immunologically demonstrable ClC-1 protein. Whereas the myotonic symptoms are severe in ADR and MTO mice and cause a considerable weight loss and reduced life span, MTO*5J mice are only mildly affected, and show less reduced body weights and near normal life spans. The physiological and histochemical properties of MTO*5J muscles are intermediate between those of ADR and wildtype control muscles. The reason for the exceptionally mild response to a complete ClC-1 deficiency is not known: removal of the transgene did not aggravate the myotonia, nor did its introduction into the MTO mouse lead to a mild phenotype. Another unusual property of MTO*5J mice is central nuclei in their muscle fibres indicating ongoing regeneration like in dystrophic muscle. Further details on the newly described MTO*5J phenotype are found in the ESI.†

Preparation of protein extracts from skeletal muscle

Freshly dissected muscle samples were quick-frozen in liquid nitrogen, transported on dry ice and stored at −80 °C prior to usage. Frozen gastrocnemius muscle specimens from 11-week old myotonic ADR, MTO, and MTO*5J mice and normal control mice were ground, in the presence of liquid nitrogen, into a fine powder using pestle and mortar. As previously described in detail,[20–22] muscle powder generated from 100 mg of wet weight tissue was resuspended in 1 ml lysis buffer containing 7 M urea, 2 M thiourea, 65 mM Chaps and 100 mM DTT, as well as 1% (v/v) ampholytes pH 4–7 or ampholytes pH 6–11. In order to eliminate excessive viscosity due to the presence of DNA, 10 µl of DNase-I was added per 1 ml of lysis buffer. The lysis buffer was also supplemented with a protease inhibitor cocktail from Roche Diagnostics (0.2 mM pefabloc, 1.4 mM pepstatin, 0.15 mM aprotinin, 0.3 mM E-64, 1 mM leupeptin, 0.5 mM soybean trypsin inhibitor and 1 mM EDTA) to avoid proteolytic degradation of skeletal muscle proteins. Following incubation for 2.3 h at 4 °C on a thermomixer with gentle shaking, the suspension was centrifuged at 4 °C for 20 min at 20 000 × *g*. The protein-containing middle layer was carefully removed. Acetone-precipitated proteins were resuspended in standard lysis buffer[21] and protein concentration was determined using a commercially available assay kit from Biorad Laboratories (Hemel-Hempstead, Herts., UK).

Two-dimensional gel electrophoretic analysis of the soluble muscle proteome

The two-dimensional gel electrophoretic separation of the urea-soluble protein complement from normal *vs.* myotonic gastrocnemius tissues was carried out using a total protein amount of 500 µg per analytical slab gel. Using a re-swelling tray from Amersham Biosciences/GE Healthcare (Little Chalfont, Bucks., UK), IPG strips of pH 4–7 and pH 6–11 were rehydrated for 12 h with 0.45 ml of a rehydration buffer containing 7 M urea, 2 M thiourea, 65 mM Chaps, 10 mg ml^{-1} DTT, and 500 µg of muscle protein sample, as well as 1% (v/v) ampholytes pH 4–7 or ampholytes pH 6–11. As a tracking dye, the buffer was complemented with 0.05% (w/v) Bromophenol Blue. Following placement of the first-dimension strips (24 cm length) gel-side up onto the Ettan IPGphor manifold and coverage with 108 ml of dry-strip cover fluid, gels were run on the IPGphor IEF system with the following isoelectric focusing running conditions: 120 min at 100 V (step and hold), 90 min at 500 V (step and hold), 60 min at 1000 V (step and hold), 60 min at 2000 V (step and hold), 60 min at 4000 V (step and hold), 120 min at 6000 V (step and hold), 240 min at 8000 V (step and hold), 180 min at 500 V (step and hold) and 240 min at 8000 V (step and hold). Following first-dimension separation, gel strips were equilibrated for 30 min. During the first 20 min of equilibration, the buffer system contained 100 mM dithiothreitol and during the last 10 min of incubation the equilibration buffer contained 0.25 M iodoacetamide. Using the EttanDalt-twelve system from Amersham Biosciences/GE Healthcare (Little Chalfont, Bucks., UK), the gel electrophoretic separation of muscle proteins in the second dimension was performed with standard 12.5% (w/v) slab gels. Following washing in SDS-containing running buffer, isoelectric focusing strips were placed on top of second dimension gels and held in place with a 1% (w/v) agarose sealing gel. Twelve slab gels were run in parallel at 0.5 W per gel for 60 min and then 15 W per gel was employed until the blue dye front had disappeared from the bottom of the gel.

Fluorescent protein labelling with RuBPs dye

Ruthenium II Bathophenathroline Disulfonate Chelate (RuBPs) staining of slab gels was carried out as previously described in detail.[23] A stock solution of RuBPs dye was prepared as outlined by Rabilloud *et al.*[24] Slab gels were fixed overnight in 30% (v/v) ethanol and 10% (v/v) acetic acid and subsequently washed 4 times with 20% (v/v) ethanol for 30 min. Gels were stained for 6 h in 20% (v/v) ethanol containing 200 nM of RuBPs dye and then re-equilibrated for 10 min in distilled water prior to image analysis. Fluorescently labeled proteins were visualised using a Typhoon Trio variable mode imager system from Amersham Biosciences/GE Healthcare (Little Chalfont, Bucks., UK). Gel analysis was performed with Progenesis SameSpots analysis software from Nonlinear Dynamics (Newcastle upon Tyne, UK) using the following parameters: ANOVA, $p < 0.05$; $n = 5$; and a power value of ≥ 0.8.[20] The 12.5% (w/v) slab gels used in this study separated muscle-associated proteins ranging in molecular mass from approximately 15 kDa to 220 kDa. Proteins in spots with a significant increase or decrease in abundance (differing between the various groups with ≥ 1.4 fold-change) were identified by mass spectrometry.

Mass spectrometric identification of muscle proteins

Excised protein spots from Coomassie Blue-stained pick gels, which were matched to RuBPs-labelled master gels, were employed for the mass spectrometric identification of proteins of interest. Standardized in-gel tryptic digestion was used for the generation of representative peptide mixtures.[21] Excision, washing, destaining and treatment with trypsin were performed by a previously optimized method.[22] Trypsin-generated peptides were harvested by removing supernatants from digested gel plugs after centrifugation. Further recovery was achieved by adding 30% acetonitrile/0.2% trifluoroacetic acid to the gel plugs for 10 min at 37 °C with gentle agitation. Resulting supernatants were pooled with the initially recovered peptides following trypsin digestion.[21] Samples were dried through vacuum centrifugation and concentrated peptide fractions were then suspended in mass spectrometry-grade distilled water and 0.1% formic acid, spun down through spin filters and added to LC-MS vials for identification by ion trap LC-MS analysis. The mass spectrometric analysis of peptides was carried out with a Model 6340 Ion Trap LC/MS apparatus from Agilent Technologies (Santa Clara, CA, USA). Separation of peptides was performed with a nanoflow Aglient 1200 series system equipped with a Zorbax 300SB C18 analytical reversed phase column using HPLC-Chip technology. Mobile phases used were A: 0.1% formic acid, B: 50% acetonitrile and 0.1% formic acid. Samples were loaded into the enrichment part of the chip at a capillary flow rate set to 4 µl min^{-1} with a mix of solvent A and solvent B at a ratio of 19 : 1. Tryptic digests were eluted with a linear gradient of 5% to 70% solvent B over 6 min, 70% to 100% solvent B over 1 min, 100% to 5% over 1 min.[22]

A 5 min post-time of solvent A was used to remove any potential carry-over. The capillary voltage was set to 2000 V. The flow and temperature of the drying gas were 4 l min^{-1} and 300 °C, respectively. Database searches were carried out with Mascot MS/MS ion search (Matrix Science, London, UK; NCBI database, release 20100212). All searches used "Mus musculus" as a taxonomic category and the following parameters: (1) two missed cleavages by trypsin, (2) mass tolerance of precursor ions ±2.5 Da and product ions ±0.7 Da, (3) carboxymethylated cysteins fixed modification, and (4) oxidation of methionine as variable modifiaction, (5) percentage coverage was set at over 10% and (6) at least 2 matched distinct peptides. Mascot scores over 48 are listed in Tables S1 to S3 (ESI†). All p*I*-values and molecular masses of identified proteins were compared to the relative position of their corresponding two dimensional spots on analytical slab gels.

Immunoblotting of muscle proteins

In order to verify alterations in the abundance of select muscle proteins and to confirm the glycolytic-to-oxidative transition process suggested by our proteomic profiling of myotonic muscle specimens, immuno-decoration of proteins of interest was performed by 1D immunoblot analysis.[22] Following the electrophoretic transfer of proteins to nitrocellulose membranes, sheets were blocked in a milk protein solution for 1 h and then incubated overnight with gentle agitation with a primary antibody, sufficiently diluted in blocking solution containing 5% (w/v) fat-free milk powder in phosphate buffered saline (PBS; 0.9% (w/v) NaCl, 50 mM sodium phosphate, pH 7.4). Subsequently, blots were washed twice with blocking solution for 10 min before incubation for 1 h with secondary peroxidase-conjugated antibodies, diluted in blocking solution. Following further washing steps with blocking solution and then two rinsing steps with PBS, antibody-decorated bands were visualized by the enhanced chemiluminescence method following the manufacturer's recommendations. Densitometric scanning of immunoblots was performed on a Molecular Dynamics 300S computing densitometer (Sunnyvale, CA, USA) with Imagequant V3.0 software.[22]

Results

This proteomic study has focused on the biochemical establishment of secondary effects of myotonia by analyzing the urea-soluble protein fraction from hyperexcitable skeletal muscle. Adult skeletal muscles are mainly composed of contractile fibres, but blood vessels, nerve fibres, connective tissue, fatty tissue, the extracellular matrix and the interstitium also contribute to muscle mass, although, under non-traumatic conditions, only to a small fraction. Thus, the varying degree of downstream alterations in the pathophysiology of ADR, MTO, and MTO*5J mice represents an ideal comparative system to determine graded myotonia-related shifts in protein expression patterns in complex muscle tissue. Comparative gel electrophoresis-based proteomic studies of crude tissue extracts typically result in the identification of soluble and relatively abundant protein species. Although two-dimensional gel electrophoresis is an excellent analytical method for the study of urea-soluble proteins,[25] the presence of certain classes of proteins is underestimated. This technical limitation has to be taken into account when one interprets proteomic data from comparative gel electrophoretic analyses. Underrepresented proteins include low-molecular-mass proteins, integral membrane proteins, extremely basic or acid proteins, and high-molecular-mass proteins.[26]

Hence, the types of proteins included in this study are urea-soluble elements that are mostly associated with the contractile apparatus, metabolic pathways, cellular signaling events and the cellular stress response. Fig. 1 and 2, as well as Tables S1 to S3 (ESI†), summarize the results of our gel electrophoresis-based proteomic investigation of potential differences in the secondary abnormalities of ADR *vs.* MTO *vs.* MTO*5J gastrocnemius muscle. In order to be able to correlate mass spectrometry-identified protein species listed in individual tables with distinct 2D protein spots of altered concentration in their respective gel images, the numbering system of proteins in tables and gels is identical with respect to ADR muscle (Fig. 1C and D; Table S1, ESI†), MTO muscle (Fig. 1E and F; Table S2, ESI†) and MTO*5J (Fig. 1G and H; Table S3, ESI†). The findings of an immunoblotting survey of alterations in the abundance of markers of glycolytic-to-oxidative transitions, as well as changes in select muscle proteins that have been identified by proteomic analysis, are presented in Fig. 3 and 4.

Proteomic profiling of ADR gastrocnemius muscle

Large-scale and high-resolution 2D gel electrophoresis, in combination with densitometric analysis using a Typhoon Trio variable imager and image analysis with Progenesis 2D analysis software, lead to the identification of 50 muscle-associated protein spots with a considerable change in concentration levels in the ADR mouse model of severe myotonia. A representative master gel with electrophoretically separated gastrocnemius muscle proteins is shown for the pH 4–7 and pH 6–11 range in Fig. 1C and D. Muscle proteins with a myotonia-related alteration in abundance ranged in molecular mass from apparent 19 kDa (myosin light chain) to 98 kDa (glycogen phosphorylase) and covered a p*I*-range from approximately 4.8 (protein disulfide isomerase) to 9.4 (troponin). The results of the mass spectrometric identification of the 50 protein species are summarized in Table S1 (ESI†), which combines data from both pH 4–7 and pH 6–11 gels. Table S1 (ESI†) lists the protein name, protein accession number, p*I*-value, molecular mass, number of matched peptide sequences, Mascot score, percentage sequence coverage, fold-change and ANOVA score of individual proteins affected by myotonia. The majority of identified proteins were shown to be constituents of the contractile apparatus, major metabolic pathways, the cellular stress response and various cellular signaling mechanisms. A reduced concentration was found for 36 muscle proteins and 14 elements were shown to be increased in their density. The muscle protein species with the highest fold decrease was identified as the phosphorylatable fast MLC2f isoform of myosin light chain. In addition to the contractile protein MLC2f (spots 1, 12, 14–17, 20), triosephosphate isomerase (spots 2, 3), 40 kDa protein (spot 4), aminoacylase (spots 5, 13), fast troponin TnI-2 (spots 6, 19), alpha-3 chain of tropomyosin (spots 7, 9), alpha and beta subunits of actin

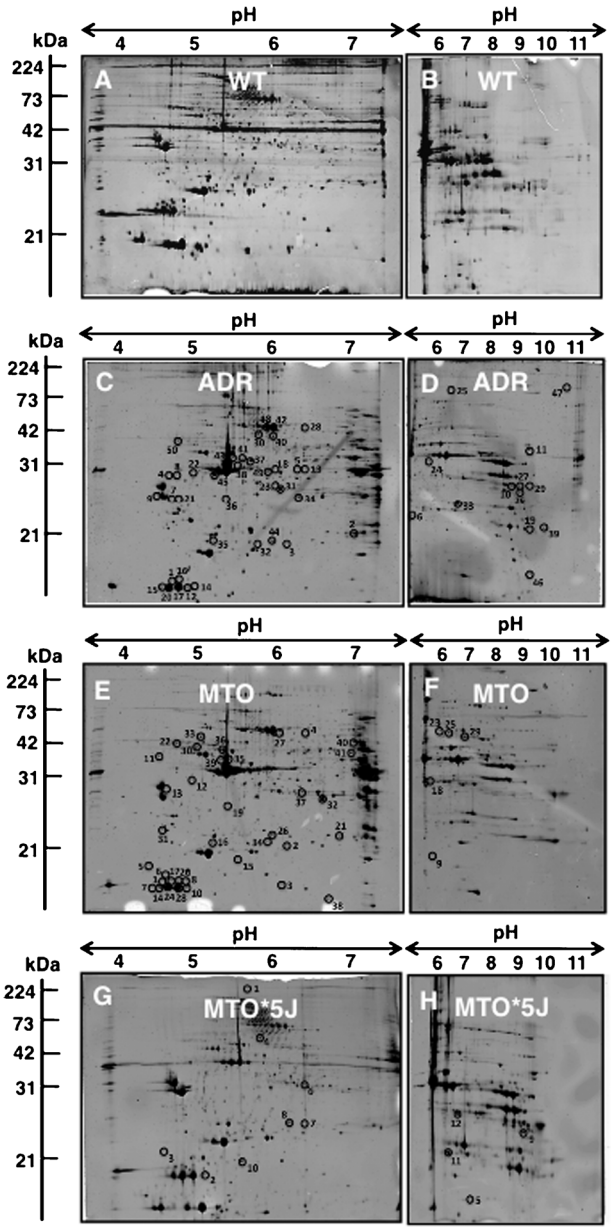

Fig. 1 Two-dimensional gel electrophoretic analysis of gastrocnemius muscle from the ADR, MTO and MTO*5J mouse model of myotonia. Shown are RuBPs-labelled master gels of muscle preparations for the pH 4–7 (A, C, E, G) and pH 6–11 (B, D, F, H) range. Wild type (WT) muscle is shown in panels A and B. Proteins with a drastically different expression level are marked by circles and are numbered 1–50 (panels C and D; ADR), 1–41 (panels E and F; MTO) and 1–12 (panels G and H; MTO*5J). See Tables S1 to S3 in the ESI† for a detailed listing of mass spectrometry-identified proteins with a changed abundance in myotonic ADR, MTO and MTO*5J muscle, respectively. The pH-values of the first dimension gel system and molecular mass standards (in kDa) of the second dimension are indicated on the top and on the left of the panels, respectively.

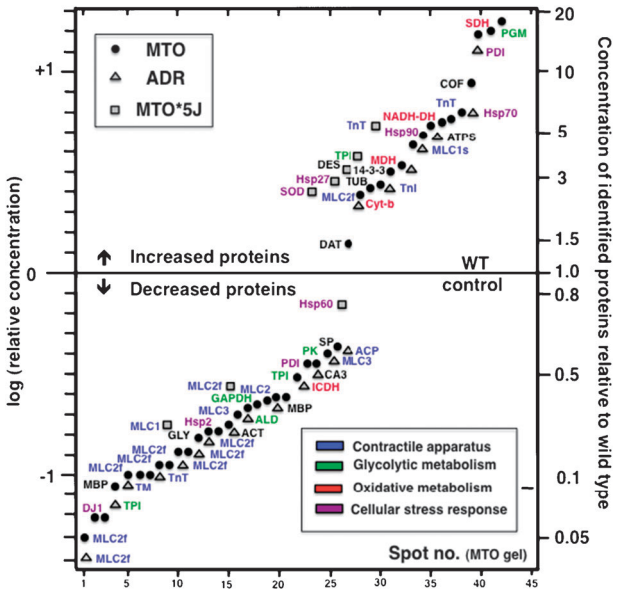

Fig. 2 Overview of alterations in ADR, MTO, and MTO*5J *vs.* wild type control muscle. The graphical presentation illustrates major changes in distinct classes of protein in hyperexcitable muscle tissues as revealed by mass spectrometry-based proteomics. The solid black spots represent MS-identified proteins with a changed abundance in MTO muscle preparations. Values for ADR muscle (triangles) and MTO*5J muscle (squares) are superimposed by their concentration relative to wild type muscle. Components belonging to the contractile apparatus, the glycolytic pathway, oxidative metabolism or the cellular stress response are marked by blue, green, red and purple symbols, respectively.

(spots 8, 18, 22), troponin TnT (spots 10, 23, 26, 27), beta subunit of trifunctional enzyme (spot 11), otubain (spot 21), aldolase (spot 24), glycogen phosphorylase (spot 25), myosin-binding protein H (spot 28), four-and-a-half-LIM-domains-1 protein (spot 29), kappa-B motif-binding proteins (spot 30), isocitrate dehydrogenase (spot 31), prosome (spot 32), carbonic anhydrase (spot 33), haloacid dehalogenase-like hydrolase (spot 34), myosin light chain isoform MLC3 (spot 35) and F-actin capping protein (spot 36) were found to be decreased in myotonic ADR muscle. In contrast, the muscle protein species with the highest fold increase was identified as the enzyme protein disulfide isomerase (spot 50). Other increased muscle proteins were represented by serpin (spot 49), heat shock protein Hsp70 (spot 48), alpha subunit of trifunctional enzyme (spot 47), mitochondrial ATP synthase (spot 46), alpha actin (spots 43 and 45), slow MLC1s isoform of myosin light chain (spot 44), albumin (spot 42), cytochrome b-c1 complex (spots 37 and 41), dihydrolipoamide *S*-acetyltransferase (spot 40), troponin TnI-2f (spot 39) and ATP-specific succinyl-CoA synthetase (spot 38).

Proteomic profiling of MTO gastrocnemius muscle

The lower and higher pH-scale of the two different IEF approaches resulted in the identification of 41 muscle protein spots with a changed abundance in the MTO mouse. A representative master gel with electrophoretically separated gastrocnemius muscle proteins is shown in Fig. 1E and F. Muscle proteins with a changed concentration covered a p*I*-range from approximately 4.6 (tropomyosin) to 7.6 (cofilin) and ranged in molecular mass from apparent 19 kDa (myosin light chain) to 84 kDa (heat shock protein Hsp90). Table S2 (ESI†) summarizes the results of the mass spectrometric identification of the 41 protein species from MTO

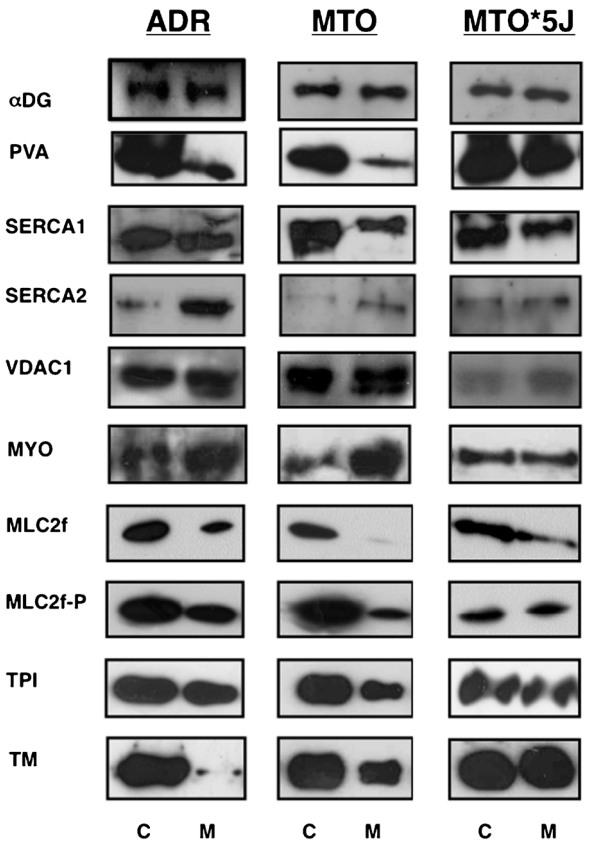

Fig. 3 Immunoblotting survey of skeletal muscle proteins with a differential expression pattern in myotonic muscle. The figure summarizes the analysis of skeletal muscle markers characteristic of a glycolytic-to-oxidative transformation process and the verification of MS-identified proteins with a changed concentration in myotonic gastrocnemius muscle. Shown is an expanded view of immuno-decorated bands from normal, ADR, MTO and MTO*5J preparations, representing α-dystroglycan (α-DG; as loading control), parvalbumin (PVA), the fast SERCA1 and slow SERCA2 isoform of the sarcoplasmic reticulum Ca^{2+}-ATPase, the voltage-dependent anion channel VDAC1, the oxygen carrier myoglobin (MYO), fast MLC2f isoform of myosin light chain, the phosphorylatable form of fast myosin light chain (MLC2f-P), the glycolytic enzyme triosephosphate isomerase (TPI) and the contractile protein tropomyosin (TM). Lanes 1 and 2 show control (C) and myotonic (M) preparations, respectively.

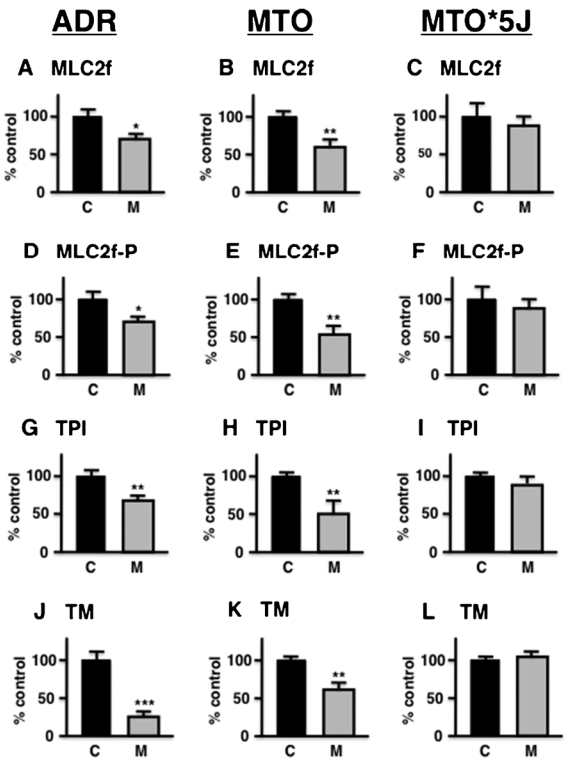

Fig. 4 Verification of select proteomic data by immunoblotting. The comparative immunoblot analysis presented in Fig. 3 was statistically evaluated using an unpaired Student's *t*-test ($n = 5$; $*p < 0.05$; $**p < 0.01$; $***p < 0.001$). The analysis of ADR, MTO and MTO*5J preparations is shown for the MLC2f isoform of myosin light chain (A–C), the phosphorylatable form of myosin light chain (MLC2f-P) (D–F), the glycolytic enzyme triosephosphate isomerase (TPI) (G–I) and the contractile protein tropomyosin (TM) (J–L). Lanes 1 and 2 show control (C) and myotonic (M) preparations, respectively.

muscle tissue. In analogy to the above-described proteins in ADR muscle, the majority of identified proteins in MTO preparations were shown to be constituents of major metabolic reactions, the contractile machinery, the cellular stress response and cell signaling pathways. An increased concentration was shown for 15 muscle proteins and 26 components were found to be decreased. As already shown for ADR muscle, the protein species with the strongest reduction was the phosphorylatable fast MLC2f isoform of myosin light chain. Decreased proteins were identified as MLC2f (spots 1, 7, 8, 10, 14, 17, 20, 24), DJ-1 protein (spot 2), heat shock protein beta-7 (spot 3), myosin-binding protein H (spot 4), T complex protein 1 (spot 5), myosin light chain MLCs (spot 6), creatine kinase (spot 9), ribonuclease/angiogenin inhibitor (spot 11), glycogenin (spot 12), tropomyosin (13), heat shock protein Hsp-2 (spot 15), myosin light chain MLC3 (spot 16), glyceraldehyde-3-phosphate dehydrogenase (spot 18), F-actin capping protein (spot 19), triosephosphate isomerase (spot 21), protein disulfide isomerase (spot 22), pyruvate kinase (spots 23 and 25) and sepiapterin reductase (spot 26). In contrast, phosphoglucomutase (spot 41) was shown to be the enzyme with the highest fold increase in MTO muscle. In addition, succinate dehydrogenase (spot 40), Actg2 protein (spot 39), cofilin (spot 38), troponin TnTf (spot 37), alpha actin (spots 35 and 36), mitochondrial NADH dehydrogenase (spot 34), heat shock protein Hsp90 (spot 33), cytosolic malate dehydrogenase (spot 32), 14-3-3 protein (spot 31), tubulin (spot 30), UTP-glucose-1-phosphate uridyltransferase (spot 29), one specific subspecies of MLC2f (spot 28) and dihydrolipoamide-*S*-acetyltransferase (spot 27) were increased in MTO gastrocnemius muscle.

Proteomic profiling of MTO*5J gastrocnemius muscle

In stark contrast to ADR and MTO muscles, the proteomic profiling of MTO*5J preparations showed considerably less changes in the degree and number of proteins. As illustrated in Fig. 1G and H, only 12 muscle protein spots with a changed abundance were identified in the MTO*5J mouse model of mild myotonia. Proteins with a changed concentration covered a p*I*-range from approximately 4.8 (myosin light chain MLC2f) to 9.2 (F1-ATP synthase) and ranged in molecular

mass from apparent 19 kDa (myosin light chain) to 61 kDa (heat shock protein Hsp60). Table S3 (ESI†) lists the names and fold-changes of the identified proteins, with 4 proteins being decreased and 8 proteins being increased in MTO*5J samples. While myosin heavy chain MHC1 (spot 1), myosin light chain MLC2f (spot 2), T complex protein 1 (spot 3) and heat shock protein Hsp60 (spot 4) were shown to be reduced, protein spots representing troponin TnTf (spots 6 and 12), triosephosphate isomerase (spot 11), desmin (spot 10), F1-ATP synthase (spot 9), NADH dehydrogenase (spot 8), heat shock protein Hsp27 (spot 7) and superoxide dismutase (spot 5) were found to be increased in MTO*5J specimens.

Overview of alterations in ADR *vs.* MTO *vs.* MTO*5J muscle

The graphical presentation of Fig. 2 gives an overview of major changes in distinct classes of protein in hyperexcitable muscle tissues as revealed by mass spectrometry-based proteomics. The solid black spots represent MS-identified proteins with a changed abundance in MTO muscle preparations. Since spot numbers and identified protein species do not correlate between individual sets of experiments (MTO *vs.* ADR *vs.* MTO*5J), the data from the other two mutants are superimposed by their concentration relative to wild type muscle. Data from ADR and MTO*5J tissue are shown by triangles and squares, respectively. Proteins belonging to the contractile apparatus, the glycolytic pathway, oxidative metabolism or the cellular stress response are marked by blue, green, red and purple symbols, respectively. The graph clearly visualizes the considerable reduction in the MLC2f isoform of myosin light chain and the metabolic trend of a glycolytic-to-oxidative transformation, as well as an increased cellular stress response in hyperexcitable muscles. The direct comparison of the 3 mutants also shows that the concentration changes in proteins are more pronounced in the severe MTO and ADR phenotypes as compared to the milder MTO*5J mouse.

Immunoblot analysis of muscle transformation in myotonia

Following the proteomic profiling of ADR, MTO and MTO*5J muscle specimens, it was essential to verify changes in select muscle proteins, as well as confirm the suggested glycolytic-to-oxidative transformation process in myotonic muscles. Immunoblotting with isoform-specific antibodies was used to determine potential changes in the protein expression profile of markers from the contractile apparatus, the regulatory machinery of excitation–contraction–relaxation cycle and energy metabolism. Antibody labeling of the surface protein α-dystroglycan was used to establish equal loading of muscle samples. Fig. 3 clearly confirms a general tendency of myotonic muscles to change to a more aerobic-oxidative phenotype in a slower-twitching fibre population. In order to correlate our immunoblotting survey to previously published work,[12] antibody labeling of parvalbumin, a well characterized high-affinity Ca^{2+}-binding protein of the sarcoplasm from fast-twitch muscle in small mammalians, was shown to be greatly reduced in ADR and MTO muscle but its concentration was only marginally affected in MTO*5J. Fibre type-specific markers of the regulatory elements of muscle relaxation, *i.e.* Ca^{2+}-ATPase isoforms SERCA1 and SERCA2, exhibited a shift from fast to slow characteristics. In addition a mitochondrial marker, VDAC1, and a marker of increased oxidative metabolism, myoglobin, were both found to be elevated in ADR and MTO mutants, but not significantly changed in the MTO*5J mouse.

In order to verify key findings from our proteomic screening of myotonic muscle preparations, 4 proteins with a changed abundance were further investigated by immunoblotting. As illustrated in Fig. 3, the MLC2f isoform of myosin light chain and the phosphorylatable MLC2f protein are greatly reduced in ADR and MTO muscle, but only marginally affected in MTO*5J preparations. This clearly confirms the proteomic findings of a reduced abundance of these contractile elements in severely myotonic muscle tissues. In addition, the remodeling of the contractile machinery, as suggested by our proteomic data, was confirmed by the abundance changes in tropomyosin in ADR and MTO preparations. Tropomyosin was shown to be considerably reduced in severely myotonic muscles. Altered expression levels of metabolic markers of anaerobic metabolism also agreed with the overall findings of the proteomic profiling of myotonic muscle. In the severely myotonic animal models ADR and MTO, a drastic decrease in the glycolytic enzyme triosephosphate isomerase was established by immunoblotting. The graphical presentation of the statistical analysis of changes in myosin light chain isoform MLC2f, the phosphorylatable form of MLC2f, triosephosphate isomerase and tropomyosin is shown in Fig. 4.

Discussion

Myotonias are intrinsic disorders of skeletal muscle[7] and characterized by uncontrolled hyperexcitability of voluntary fibres.[3] Since long-term muscle activity influences the concentration of many proteins in contractile fibres,[27–30] it was of interest to study potential global changes in the skeletal muscle proteome due to myotonic pathology. The comparative proteomic profiling of the myotonic animal models ADR, MTO and MTO*5J clearly revealed a drastically perturbed protein expression pattern in the severely affected ADR and MTO muscle, but only moderate changes in mildly diseased MTO*5J animals. Hence, the severity of myotonic symptoms appears to correlate well with the quantitative and qualitative alterations in the protein complement of ADR and MTO *vs.* MTO*5J muscle tissues. Skeletal muscles from the ADR and MTO phenotype appear to be associated with considerable myotonia-related changes in proteins involved in the excitation–contraction–relaxation cycle, energy metabolism, ion handling, stress response and cellular signaling. A striking feature in both animal models was the drastic decrease in almost all subspecies of the phosphorylatable fast MLC2f isoform of myosin light chain, which agrees with previous biochemical studies of the ADR mouse.[12,14,15]

Drastic reduction in fast myosin light chain MLC2f

Previous proteomic studies have shown that isoform changes in myosin light chains represent reliable markers of muscle transformation.[31] Chronic low-frequency stimulation of fast rabbit muscle triggers a significant decrease in various MLCf molecules and an increase in slower counterparts.[20,32]

A drastic increase of slow myosin light chain MLC2s was observed in senescent rat skeletal muscle, which is indicative of an increased slow fibre population in sarcopenia of old age.[33] In analogy, the reduced density of 7, 8 and 1 subspecies of MLC2f in ADR, MTO and MTO*5J muscle preparations, respectively, strongly suggests a partial fast-to-slow transition process in myotonia. In addition, this finding confirms the idea that enhanced neuromuscular activity regulates the abundance of this contractile protein.[14] Proteomics revealed a concomitant 4-fold increase in the slow MLC1s isoform of myosin light chain in ADR muscle. Thus, myotonia is clearly associated with a distinct muscle transformation process. Differential effects on troponins and a reduction of tropomyosin, F-actin capping protein and myosin-binding protein H in MTO and ADR muscle tissue agree with the idea of a myotonia-induced process of extensive fibre remodeling.

Myotonia-related changes in metabolic enzymes

Many metabolic enzymes are thought to be multi-functional,[34] which makes the proteomic interpretation of differential changes in glycolytic enzymes, mitochondrial components and metabolite transporters sometimes difficult.[35] Despite the fact that these biochemical facts have to be properly taken into account, the present study clearly showed a general trend of decreased glycolytic and anaerobic markers *vs.* an increase in mitochondrial and oxidative indicator molecules in myotonia. The decrease in triosephosphate isomerase, aldolase and glycogen phosphorylase on the one hand and a concomitant increase in mitochondrial ATP synthase, albumin, isocitrate dehydrogenase dihydrolipoamide *S*-acetyltransferase, ATP-specific succinyl-CoA synthetase and cytochrome b-c1 complex in ADR suggested a reduced utilization of glucose and increased fatty acid oxidation and mitochondrial metabolism. In analogy, a decrease in glyceraldehyde-3-phosphate dehydrogenase, triosephosphate isomerase and pyruvate kinase and an increase in succinate dehydrogenase, NADH dehydrogenase and albumin in MTO agreed with a myotonia-dependent glycolytic-to-oxidative transition mechanism. However, there was an increase in phosphoglucomutase, which might be due to the multi-functional nature of this glycolytic element.[34]

Muscle type transformation in myotonia

Immunoblotting supported major findings of our mass spectrometry-based proteomic study. Antibody labeling confirmed a switch from the fast SERCA1 isoform of the sarcoplasmic reticulum Ca^{2+}-pump to its slower SERCA2 form. This agrees with the idea of myotonia-induced muscle transformation at the level of physiological handling of Ca^{2+}-homeostasis. The comparative immunoblot survey presented here demonstrated reduced levels of parvalbumin in ADR and MTO tissue that agrees with previous studies.[14,15] A considerably less pronounced reduction of parvalbumin was observed in the milder MTO*5J phenotype. Since it is well established that the parvalbumin content is significantly different between predominantly glycolytic *vs.* oxidative fibres,[36,37] this cytosolic Ca^{2+}-binding protein might be employable as a reliable general marker of the severity of myotonia.[15] The striking red colour of ADR and MTO myotonic gastrocnemius muscles is probably in large part due to increased myoglobin levels, as suggested by immunoblotting in this report. This drastic increase in myoglobin has also been reported to occur in fast muscle following chronic electro-stimulation,[20,32] which makes this essential oxygen-carrier probably a crucial limiting factor of the metabolic switch to more oxidative metabolism in skeletal muscles.[38] Hence, distinct isoform switches in fast and slow subspecies of myosin light chain and partially myosin heavy chains,[18] as well as a drastic decrease in parvalbumin and a considerable increase in myoglobin and VDAC1 represent a set of biochemical changes indicative of myotonia.

Potential new biomarkers of myotonia

In addition to the above-discussed alterations in common fibre type-specific markers, many other interesting changes in distinct protein species occurred in the myotonic animal models studied here by proteomics. The decrease of 40 kDa protein, aminoacylase, otubain, four-and-a-half-LIM-domains-1 protein, kappa-B motif-binding protein, growth factor receptor bound protein 2, prosome, carbonic anhydrase and haloacid dehalogenase-like hydrolase in ADR muscle indicates impairments in metabolism of amino groups, deubiquitination, gene transcription, signal transduction, differentiation, CO_2-removal, and carbon or phosphoryl group transfer. Increases in serpin and heat shock protein Hsp70 may be associated with changes in protease inhibition and cellular stress response. These proteins represent a large number of novel potential biomarkers for ADR muscle changes. The reduced density of carbonic anhydrase isoform CA3 could be interpreted as a potential impairment of the CO_2-removal mechanism in myotonia. Carbonic anhydrase converts CO_2 into carbonic acid,[39] therefore its lower expression levels may trigger a reduced availability of this essential hydration reaction which may result in harmful levels of CO_2 in myotonic fibres. Interestingly, in the case of the trifunctional enzyme its beta subunit was reduced and its alpha subunit increased in ADR muscle preparations. Further biochemical studies are needed to be able to interpret the effects of these changes on mitochondrial metabolism.

In MTO muscle, the decrease in heat shock protein beta-7, T complex protein 1, creatine kinase M-type, ribonuclease/angiogenin inhibitor, glycogenin, heat shock protein Hsp-2 and sepiapterin reductase indicates a partially reduced activity of the cellular stress response, the creatine shuttle system, regulation of neovascularization, glucose metabolism and amino acid metabolism. The increase in Actg2 protein, heat shock protein Hsp90, 14-3-3 protein, tubulin, UTP-glucose-1-phosphate uridyltransferase might also be of considerable importance for the future establishment of a comprehensive biomarker signature of myotonia. The elevated levels of these muscle-associated elements could trigger changes in actin organization, cellular stress response, DNA replication, microtubular assembly and glucose metabolism. The enzyme protein disulfide isomerase was shown to be increased in ADR muscle, but decreased in MTO, and could thus be potentially used as a differentiating marker of these two different myotonic phenotypes. This thiol-disulfide oxidoreductase of the sarcoplasmic reticulum catalyzes the exchange of a disulfide bond

with substrates thereby facilitating correct protein folding.[40] The mildest phenotype studied, gastrocnemius muscle from MTO*5J mice, showed only a moderate decrease in myosin heavy chain MHC1, myosin light chain MLC2f, T complex protein 1 and heat shock protein Hsp60 and an increase in troponin TnTf, triosephosphate isomerase, desmin, F1-ATP synthase, NADH dehydrogenase, heat shock protein Hsp27 and superoxide dismutase. This finding indicates that the milder disease progression is associated with less pronounced downstream effects on the global muscle protein complement.

Limitations of gel electrophoresis-based proteomics

Since the concentration range of proteins is not a static entity, but highly dynamic, and because the density of proteins spans several orders of magnitude in complex cellular systems, no biochemical technique is capable of determining concentration changes in all components belonging to a given proteome. Therefore, studies on urea-soluble muscle proteins by two-dimensional gel electrophoresis, as described here, focus mostly on proteins that are associated with the contractile apparatus, metabolic pathways and the cellular stress response. Proteins such as myosin heavy chains, parvalbumin and the muscular chloride channel were not covered in our 2D gel electrophoretic approach probably due to their high molecular mass, low molecular mass or low abundance, respectively. In addition, the densitometric analysis of highly abundant proteins is often complicated by excessive streaking and cross-contaminations between crowded spot regions. Multiple spots of the same protein species may be due to primary products of slightly different isogenes or because of secondary modifications, such as phosphorylation.

Conclusion

Over the last few years, mass spectrometry-based proteomics has been applied to the large-scale study of fibre-associated changes in established animal models of myogenesis, muscle differentiation, muscular disorders and natural aging.[31] In analogy, here we have analysed the myotonic mouse models ADR, MTO and MTO*5J using fluorescent 2D gel electrophoresis and mass spectrometry to identify novel protein markers of myotonia-related changes. Myotonia appears to trigger considerable changes in many elements of the contractile apparatus, cellular processes and muscle energy metabolism. A detailed biochemical, cell biological and physiological characterization of these new biomarkers in the future will hopefully improve our general understanding of the molecular pathogenesis of myotonia. Fig. 5 summarizes major events in the molecular pathogenesis of myotonia and key findings from our proteomic survey. Destabilization of the membrane potential due to the loss of sarcolemmal Cl^- conductance triggers hyperexcitability of skeletal muscle fibres in myotonia. Muscle cramps and drastically increased intracellular Ca^{2+} levels, resulting from unscheduled bursts of action potentials,

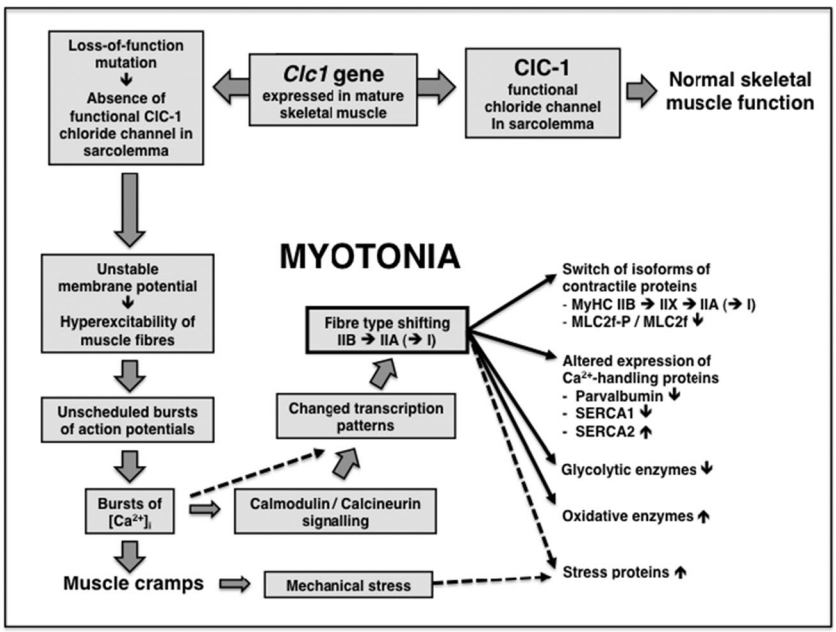

Fig. 5 Myotonia: from single gene defect to a plethora of secondary changes in the skeletal muscle phenotype. A single nucleotide replacement or other event at the DNA level in the *Clc1* gene is sufficient to cause loss of function of the muscular chloride channel ClC-1. In mammals, ClC-1 is expressed in the sarcolemma of mature skeletal muscle, and is required for normal function. Loss of sarcolemmal Cl^- conductance destabilizes the membrane potential and leads to hyperexcitability of the muscle fibre, the hallmark of myotonia (generalized myotonia in humans). Unscheduled bursts of action potentials cause bursts of intracellular Ca^{2+} release and cramps. Elevated intracellular Ca^{2+} activates Ca^{2+}-dependent signalling pathways, *e.g.* those involving calmodulin/calcineurin and NFAT (nuclear factor of activated T-cells), as shown for the genes for myosin heavy chains. In myotonic mouse muscles, there is a fibre type shift from fast glycolytic (type IIB) to fast oxidative (type IIA), partially even to type I (slow) involving changes in key metabolic enzymes and Ca^{2+}-handling proteins like parvalbumin. Presumably due to cramps and imbalance of gene expression, there is a considerable cellular stress response in myotonic muscle fibres. Dashed arrows symbolize pathways that are not well characterized.

cause an increased cellular stress response and activation of Ca^{2+}-dependent signalling pathways, respectively.[41,42] Fibre type shifting and increased expression levels of mitochondrial enzymes in myotonic mouse muscles were confirmed by proteomics. Fibre type transitions from fast-glycolytic to fast-oxidative fibres are concomitant with altered concentrations in glycolytic enzymes, mitochondrial components and Ca^{2+}-handling proteins.[13–18] An increased density of mitochondria and satellite cells was previously reported in myotonic muscle.[43] Myotonia appears to have differential effects on various elements of the cellular stress response. Proteomics clearly revealed elevated levels of the molecular chaperones Hsp27, Hsp70 and Hsp90 in affected muscle tissue. In conclusion, our proteomic profiling study has shown that a single mutation in a muscle-specific gene that triggers hyper-excitability of the sarcolemma has severe downstream effects on the expression levels of a very large number of genes in contractile tissues, showing the extreme complexity of gene regulation in skeletal muscle.

Acknowledgements

Research was funded by the Irish Health Research Board (HRB-RP/2008/1) and Fonds der Chemischen Industrie (FCI). The authors thank Dr Peter Heimann (Department of Cell Biology, University of Bielefeld, Germany) for his generous help in preparing myotonic mouse muscle. The Irish Higher Education Authority and the Deutscher Akademischer Austauschdienst supported several laboratory visits of the Maynooth team to Bielefeld.

References

1 K. Jurkat-Rott, H. Lerche and F. Lehmann-Horn, *J. Neurol.*, 2002, **249**, 1493–1502.
2 R. Rüdel and F. Lehmann-Horn, *Physiol. Rev.*, 1985, **65**, 310–356.
3 E. Matthews, D. Fialho, S. V. Tan, S. L. Venance, S. C. Cannon, D. Sternberg, B. Fontaine, A. A. Amato, R. J. Barohn, R. C. Griggs, M. G. Hanna and CINCH Investigators, *Brain*, 2010, **133**, 9–22.
4 R. Planells-Cases and T. J. Jentsch, *Biochim. Biophys. Acta*, 2009, **1792**, 173–89.
5 C. Lossin and A. L. George Jr., *Adv. Genet.*, 2008, **63**, 25–55.
6 P. Doran, K. O'Connell, J. Gannon and K. Ohlendieck, *Proteomics: Clin. Appl.*, 2007, **1**, 1169–1184.
7 E. M. Füchtbauer, J. Reininghaus and H. Jockusch, *Proc. Natl. Acad. Sci. U. S. A.*, 1988, **85**, 3880–3884.
8 K. Steinmeyer, R. Klocke, C. Ortland, M. Gronemeier, H. Jockusch, S. Gründer and T. J. Jentsch, *Nature*, 1991, **354**, 304–308.
9 G. Mehrke, H. Brinkmeier and H. Jockusch, *Muscle Nerve*, 1988, **11**, 440–446.
10 R. L. Watts, J. Watkins and D. C. Watts, in *The Biochemistry of Myasthenia Gravis and Muscular Dystrophy*, ed. R. Marchbanks and G. Lunt, Academic, London, 1978, pp. 331–334.
11 M. Gronemeier, A. Condie, J. Prosser, K. Steinmeyer, T. J. Jentsch and H. Jockusch, *J. Biol. Chem.*, 1994, **269**, 5963–5967.
12 I. Stuhlfauth, J. Reininghaus, H. Jockusch and C. W. Heizmann, *Proc. Natl. Acad. Sci. U. S. A.*, 1984, **81**, 4814–4818.
13 J. Reininghaus, E. M. Füchtbauer, K. Bertram and H. Jockusch, *Muscle Nerve*, 1988, **11**, 433–439.
14 H. Jockusch, J. Reininghaus, I. Stuhlfauth and M. Zippel, *Eur. J. Biochem.*, 1988, **171**, 101–105.
15 F. W. Kluxen, F. Schöffl, M. W. Berchtold and H. Jockusch, *Eur. J. Biochem.*, 1988, **176**, 153–158.
16 M. Schleef, C. Zühlke, F. Schöffl and H. Jockusch, *Neuromuscular Disord.*, 1994, **4**, 205–217.
17 R. Klocke, K. Steinmeyer, T. J. Jentsch and H. Jockusch, *J. Biol. Chem.*, 1994, **269**, 27635–27639.
18 O. Agbulut, P. Noirez, G. Butler-Browne and H. Jockusch, *FEBS Lett.*, 2004, **561**, 191–194.
19 D. Pette and R. S. Staron, *Histochem. Cell Biol.*, 2001, **115**, 359–372.
20 P. Donoghue, P. Doran, K. Wynne, K. Pedersen, M. J. Dunn and K. Ohlendieck, *Proteomics*, 2007, **7**, 3417–3430.
21 P. Doran, G. Martin, P. Dowling, H. Jockusch and K. Ohlendieck, *Proteomics*, 2006, **6**, 4610–4621.
22 K. O'Connell and K. Ohlendieck, *Proteomics*, 2009, **9**, 5509–5524.
23 J. Gannon, L. Staunton, K. O'Connell, P. Doran and K. Ohlendieck, *Int. J. Mol. Med.*, 2008, **22**, 33–42.
24 T. Rabilloud, J. M. Strub, S. Luche, A. van Dorsselaer and J. Lunardi, *Proteomics*, 2001, **1**, 699–704.
25 W. Weiss and A. Görg, *Methods Mol. Biol.*, 2009, **564**, 13–32.
26 T. Rabilloud, M. Chevallet, S. Luche and C. Lelong, *J. Proteomics*, 2010, **73**, 2064–2077.
27 H. Reichmann, R. Wasl, J. A. Simoneau and D. Pette, *Pfluegers Arch.*, 1991, **418**, 572–574.
28 A. Hicks, K. Ohlendieck, S. O. Göpel and D. Pette, *Am. J. Physiol.*, 1997, **2273**, C297–C305.
29 G. R. Froemming, B. E. Murray, S. Harmon, D. Pette and K. Ohlendieck, *Biochim. Biophys. Acta*, 2000, **1466**, 151–168.
30 V. Ljubicic, P. J. Adhihetty and D. A. Hood, *Can. J. Appl. Physiol.*, 2005, **30**, 625–643.
31 K. Ohlendieck, *Expert Rev. Proteomics*, 2010, **7**, 283–296.
32 P. Donoghue, P. Doran, P. Dowling and K. Ohlendieck, *Biochim. Biophys. Acta*, 2005, **1752**, 166–176.
33 J. Gannon, P. Doran, A. Kirwan and K. Ohlendieck, *Eur. J. Cell Biol.*, 2009, **88**, 685–700.
34 J. W. Kim and C. V. Dang, *Trends Biochem. Sci.*, 2005, **30**, 142–150.
35 K. Ohlendieck, *Biochim. Biophys. Acta*, 2010, **1804**, 2089–2101.
36 T. L. Schmitt and D. Pette, *Histochemistry*, 1991, **96**, 459–465.
37 B. Huber and D. Pette, *Eur. J. Biochem.*, 1996, **236**, 814–819.
38 M. Kaufmann, J. A. Simoneau, J. H. Veerkamp and D. Pette, *FEBS Lett.*, 1989, **245**, 181–184.
39 C. Geers and G. Gros, *Physiol. Rev.*, 2000, **80**, 681–715.
40 C. Appenzeller-Herzog and L. Ellgaard, *Biochim. Biophys. Acta*, 2008, **1783**, 535–548.
41 Z. A. Ran, K. Gundersen and A. Buonanno, *Proc. Natl. Acad. Sci. U. S. A.*, 2008, **105**, 5921–5926.
42 E. Calabria, S. Ciciliot, I. Moretti, M. Garcia, A. Picard, K. A. Dyar, G. Pallafacchina, J. Tothova, S. Schiaffino and M. Murgia, *Proc. Natl. Acad. Sci. U. S. A.*, 2009, **106**, 13335–13340.
43 J. Schimmelpfeng, H. Jockusch and P. Heimann, *Cell Tissue Res.*, 1987, **249**, 351–357.